

NACA RM E56L07

8669



Reg # 6692

# RESEARCH MEMORANDUM

MAR 6 - 1957

DESIGN AND TEST OF MIXED-FLOW IMPELLERS

VIII - COMPARISON OF EXPERIMENTAL RESULTS FOR THREE  
IMPELLERS WITH SHROUD REDESIGNED BY RAPID

APPROXIMATE METHOD

By Walter M. Osborn, Kenneth J. Smith, and Joseph T. Hamrick

Lewis Flight Propulsion Laboratory  
Cleveland, OhioTECH LIBRARY KAFB, NM  
0143995

  
NATIONAL ADVISORY COMMITTEE  
FOR AERONAUTICS

WASHINGTON

February 27, 1957





## NATIONAL ADVISORY COMMITTEE FOR AERONAUTICS

RESEARCH MEMORANDUM

## DESIGN AND TEST OF MIXED-FLOW IMPELLERS

## VIII.- COMPARISON OF EXPERIMENTAL RESULTS FOR THREE IMPELLERS

## WITH SHROUD REDESIGNED BY RAPID APPROXIMATE METHOD

By Walter M. Osborn, Kenneth J. Smith, and Joseph T. Hamrick

## SUMMARY

Three centrifugal impellers with parabolic, circular, and skewed-parabolic blading were modified by a recently developed design procedure to reduce the velocity gradients along the hub from inlet to outlet. All original dimensions except the shroud contours were retained. Experimental investigation showed that the modified impellers had better performance characteristics than the original impellers at all speeds investigated, the greatest gains occurring at speeds of 1300 feet per second and higher. These large gains probably resulted primarily from more favorable velocity gradients and from designing these impellers further away from the condition necessary for eddy formation. The modified impellers were thus able to operate over a wider range of weight flows at high speeds.

The modified impellers were investigated over a range of equivalent speeds of 900 to 1500 feet per second and flow rates from maximum to the point of incipient surge. At 1300 feet per second, the peak pressure ratio and maximum adiabatic temperature-rise efficiency for the parabolic-bladed impeller were 3.07 and 0.825, respectively. For the same conditions, the circular-bladed impeller and the skewed-parabolic-bladed impeller had pressure ratios of 3.13 and 3.15 and efficiencies of 0.737 and 0.805, respectively. Of the three, the parabolic-bladed impeller had the highest maximum efficiencies (0.854 to 0.800) and the best weight-flow range over the speed range tested. On the basis of the parameters investigated, it appears that parabolic blading is superior to circular blading. The experimental results indicate that the design method of NACA TN 3399 is a reliable method for use in designing centrifugal impellers.

## INTRODUCTION

Prior to 1947 a series of mixed-flow centrifugal impellers were built and tested at the NACA Lewis Laboratory. All impellers of this series, three of which are reported in reference 1, exhibited severe flow instabilities at impeller tip speeds above 1300 feet per second and moderate

instabilities at lower speeds. In 1949, a flow analysis for one of these impellers (parabolic-bladed) was made and reported in reference 2. The analysis indicated that there were large decelerations in flow along the impeller hub. Such decelerations probably contributed to flow separation and were responsible in part for the low efficiency of the impeller. Further analysis in the blade-to-blade plane showed large potential-flow eddies on the driving face of the impeller blade. With such eddies in viscous flow, it was considered improbable that the flow would be steady. It was believed that the flow would separate if the eddies started to form or that there would be flow separation due to the large decelerations that generally occur before eddy formation. Separation in any one passage could cause stalling with blockage of the passage and subsequent diversion of the flow to adjacent passages. Such an occurrence could result in rotating stall, as discussed in reference 3, even when the angle of flow into the blade inlet is optimum. A rotating-stall condition should be avoided, as it may be one of the devices that trigger violent surge.

In 1954, a method was developed for the design of hub-shroud profiles for centrifugal impellers of a given blade shape (ref. 4). In order to test the reliability of the newly developed design method, the shroud profile of the parabolic-bladed impeller was redesigned so as to allow little or no deceleration on the hub and eliminate potential-flow eddies on the blade driving face. The details of the redesign are reported in reference 4 (parabolic-bladed impeller of this report), and the experimental results are reported in reference 5. Because of the great improvement obtained with this impeller, it was decided to modify two additional impellers of the original series in order to determine the effect on their performance of reducing the velocity gradients and of reducing or eliminating the eddy, thus testing further the reliability of the design method. In addition, it was expected that further information on the effect of blade-loading distribution would be obtained. One of these impellers was the circular-bladed impeller of reference 1. The other impeller was a skewed-parabolic-bladed impeller for which the experimental results were not previously reported. The shroud shapes for the two additional impellers were redesigned, and the impellers were tested at the NACA Lewis laboratory.

The experimental results in air for the three redesigned impellers are presented herein and are analyzed and compared with the experimental results of the impellers as originally designed.

#### SYMBOLS

- L fraction of total streamline length from impeller inlet
- Q ratio of velocity relative to impeller to stagnation speed of sound upstream of impeller inlet
- U actual impeller tip speed, ft/sec

- w actual air weight flow, lb/sec
- $\gamma$  ratio of specific heats
- $\delta$  ratio of inlet total pressure to NACA standard sea-level pressure of 29.92 in. Hg abs
- $\eta_{ad}$  adiabatic temperature-rise efficiency
- $\theta$  ratio of inlet total temperature to NACA standard sea-level temperature of 518.7° R

## THEORETICAL DESIGN

Three centrifugal impellers with parabolic, circular, and skewed-parabolic blading were modified by the method presented in reference 4. The original hub profile, blade curvature, and blade thickness were maintained; and the velocities were controlled by redesigning the shroud. The parabolic-bladed impeller is the example impeller in reference 4; the design procedures for the circular- and skewed-parabolic-bladed impellers were the same as for the parabolic-bladed impeller. The three impellers were redesigned to reduce the flow decelerations along the hub and also to avoid a potential-flow eddy on the driving face of the blade. Eddy formation is taken herein as beginning when the theoretical velocity on the blade surface becomes negative. The design operating conditions for the impellers were chosen as follows:

Equivalent impeller tip speed, $U/\sqrt{\theta}$ , ft/sec . . . . .	1331
Ratio of specific heats, $\gamma$ . . . . .	1.4
Prerotation . . . . .	0
Flow direction at outlet . . . . .	Radial

Figures 1(a), (b), and (c) show the assigned hub velocities and the resulting shroud velocities for the redesigned (isentropic) parabolic-, circular-, and skewed-parabolic-bladed impellers, respectively. The hub velocities for the original parabolic-bladed impeller are also shown in figure 1(a). The deceleration of the flow along the hub from the inlet to the midsection of the impeller is considerably reduced for the redesigned parabolic-bladed impeller (as compared with the original impeller). The flow then accelerates from the midsection to the outlet. It is probable that the redesigned circular- and skewed-parabolic-bladed impellers are similarly improved. The circular- and skewed-parabolic-bladed impellers have the same assigned hub velocities.

Figure 2 shows the redesigned (isentropic) hub-shroud profiles with contours of constant velocity ratio  $Q$ . Also shown are the original shroud profile and the modified shroud profile. The modified shroud profile consists of the isentropic design shroud plus an allowance for boundary layer and losses and is the shroud for which the experimental results

are presented in this report. The allowance for boundary layer and losses was based upon experience obtained from an investigation of mixed-flow impellers conducted at the NACA Lewis Laboratory from 1950 to 1955 and reported in references 5 to 12. The boundary-layer allowance for the modified parabolic-bladed impeller was 30 percent of the blade height at outlet and varied linearly with distance along the shroud to zero at the impeller inlet. The test results for this impeller (ref. 5) indicate that this allowance is too small for this impeller at design speed. Therefore, the boundary-layer allowance for the circular- and skewed-parabolic-bladed impellers was increased to 40 percent of the blade height at the outlet.

Figure 2(b) shows that the shroud profile for the circular-bladed impeller has a slight dip near the inlet. The size of this dip depends upon the velocity assigned at the hub near the impeller inlet. By assigning increasing velocities in this region, the dip became so large that a two-piece shroud or a fully shrouded impeller would have been necessary for assembly. By assigning slightly decreasing velocities, the dip became tolerable, and it was possible to use a one-piece shroud. This condition was also found in the design of the parabolic- and skewed-parabolic-bladed impellers and accounts for the slightly decelerating flow that was assigned to the inlet portions of the three impellers at the hub (fig. 1). In a design in which there was freedom to change the hub shape, the accelerating flow could be retained and the hub shape changed to eliminate the dip. Some adjustment could also be made by varying the blade thickness.

The velocity distribution in the blade-to-blade plane for the redesigned (isentropic) parabolic-bladed impeller is presented in figure 3. Also shown in figure 3(a) is the velocity distribution for the original parabolic-bladed impeller. This impeller was designed with a five-stream-tube (hub-shroud) solution and a three-stream-tube solution. There was no significant difference between the two solutions. The circular- and skewed-parabolic-bladed impellers were designed using three stream tubes. Figure 3 indicates that the redesign of the parabolic-bladed impeller resulted in a flow that was not near the theoretical condition necessary for formation of a potential-flow eddy (a condition that was present in the original impeller, fig. 3(a)). This was accomplished by increasing the velocity ratio from 0.17 to 0.55 (fig. 1(a)) in the region where the eddy occurs.

Figure 3 also shows that the parabolic-bladed impeller is very lightly loaded (small difference between driving- and trailing-face velocities) from the inlet to approximately 0.4 L. On the basis of this low blade loading, this impeller was also tested with every other blade cut back to form splitter vanes, and the results are presented in reference 11.

Figures 4 and 5 show the velocity distribution in the blade-to-blade plane for the redesigned (isentropic) circular- and skewed-parabolic-bladed impellers, respectively. The blade loadings for the two impellers

indicate that the skewed-parabolic-bladed impeller is more lightly loaded in the inlet section of the impeller than is the circular-bladed impeller. These impellers also avoid the theoretical condition necessary for formation of a potential-flow eddy; however, they approach this condition more closely than does the parabolic-bladed impeller. In the design of the modified circular- and skewed-parabolic-bladed impellers, the blades were treated as if they contained radial blade elements for ease in determining the geometric parameters. The effect of this assumption upon the design is not known.

## APPARATUS, INSTRUMENTATION, AND PROCEDURE

### Apparatus

Three centrifugal impellers designed in 1947 with parabolic, circular, and skewed-parabolic blading were used in this investigation. The shrouds were modified as discussed previously. The outlet diameter of each impeller was 12.0 inches. Photographs of the three impellers are shown in figure 6. Each impeller had 18 blades, and all original dimensions except the shroud contours were maintained. The original and modified shrouds for the three impellers are shown in figure 2. The design technique and experimental results for the original parabolic- and circular-bladed impellers are presented in reference 1, and some of the experimental results are repeated in this report for comparison with the modified design. Experimental data for the original skewed-parabolic-bladed impeller are available and are also presented herein for comparison with the modified impeller.

The parabolic-bladed impeller had radial blade elements. The blade curvature corresponds to that of a parabola on the developed surface of a cylinder. This curvature extends the full depth of the impeller and is so oriented that a particle following the blade with a constant axial velocity would have a constant angular acceleration. The coordinates for the modified impeller shroud and design information are given in references 5 and 1.

The circular-bladed impeller had nonradial blade elements that were inclined in the direction of rotation  $7.5^\circ$  to a radial line at the impeller discharge. The inlet portion of the blade surfaces for the first 60 percent of the impeller axial depth generates a circular cylinder, and the remainder of the blade surface generates a plane tangent to the circular cylinder.

The skewed-parabolic-bladed impeller had nonradial blade elements. The driving side of the blade was formed by holding the cutter at an angle of  $15^\circ$  to the meridional plane; for the trailing side of the blade, the cutter was held at an angle of  $16^\circ$ . Thus, the parabolic blade shape for

this impeller becomes skewed as compared with the parabolic-bladed impeller, in which the cutter was in the meridional plane and formed radial blade elements.

The three impellers were tested with a 25-inch-diameter vaneless diffuser of constant area in the radial direction. The rear diffuser wall was the same for the three impellers, but the front diffuser wall was different for each impeller because of the difference in blade height at the outlet of the three impellers. There was approximately 0.040-inch clearance (normal to impeller shroud) between the impeller and the shroud wall with the impeller in a stationary position. A schematic diagram of the modified parabolic-bladed impeller and diffuser is shown in figure 7. The circular- and skewed-parabolic-bladed installations were similar.

Adapters were made for the front and rear of the impellers to fit to the existing shafting, the impeller being straddle-mounted between two bearings. This differs from the original installation (ref. 1), in which the impeller was supported by a rear bearing only (overhung). Thus, in the installation of reference 1, the radius of the outer wall was constant upstream of the inlet and converged at the inner radius (spinner); whereas, for the present installation, the radius of the inner wall is constant and the outer wall radius converges as shown in figure 7. The effect of this difference of inlet geometry on the performance of the impeller is unknown.

The remainder of the experimental setup is the same as that described in reference 7.

#### Instrumentation

The instrumentation is similar to that described in reference 7. The outlet measuring station is located at a 12-inch radius (twice the impeller-outlet radius) in the vaneless diffuser, as shown in figure 7, and is at the same radius as in the original installation of reference 1. The diffuser instrumentation consisted of eight static-pressure taps, four thermocouple rakes, and 12 total-pressure probes. Four static-pressure taps were located in the front diffuser wall at 90° intervals around the annulus opposite four static-pressure taps in the rear diffuser wall. The four thermocouple rakes were also placed 90° apart and had three thermocouples per rake spaced at intervals of 1/6, 1/2, and 5/6 of the distance across the passage. The 12 total-pressure probes were distributed around the annulus to give a coverage for total pressure equivalent to that of the temperature measurements. In addition, 11 static taps were located along the shroud wall from the impeller inlet to the outlet.

### Procedure

This investigation was carried out at a constant inlet-air pressure of 20 inches of mercury absolute. The inlet temperatures varied from ambient to  $-55^{\circ}$  F. The flow rate was varied from maximum to the point of incipient surge by varying the outlet pressure. The impeller equivalent speed was varied from 900 to 1500 feet per second based on an impeller-outlet radius of 6 inches. The test and computational procedures are the same as those used in reference 7.

### EXPERIMENTAL RESULTS

The over-all performance characteristics for the three modified impellers are based on measurements taken at twice the impeller-outlet radius in a vaneless diffuser.

#### Modified Parabolic-Bladed Impeller

The over-all performance characteristics for the modified parabolic-bladed impeller are presented in figure 8 for a range of speed from 900 to 1500 feet per second. The peak pressure ratio and maximum adiabatic efficiency at 1300-feet-per-second equivalent speed were 3.07 and 0.825, respectively. At the maximum speed of 1500 feet per second, the peak pressure ratio was 4.03 and the maximum efficiency was 0.800. The average Mach number at the outlet measuring station for the maximum-efficiency points over the range of speed was between 0.36 and 0.44.

#### Modified Circular-Bladed Impeller

The over-all performance characteristics for the modified circular-bladed impeller are presented in figure 9 for a range of speed from 900 to 1500 feet per second. The peak pressure ratio and maximum adiabatic efficiency at 1300-feet-per-second equivalent speed were 3.13 and 0.737, respectively. At the maximum speed of 1500 feet per second, the peak pressure ratio was 3.75 and the maximum efficiency was 0.658. The average Mach number at the outlet measuring station for the maximum-efficiency points over the range of speed was between 0.41 and 0.61.

#### Modified Skewed-Parabolic-Bladed Impeller

The over-all performance characteristics for the modified skewed-parabolic-bladed impeller are presented in figure 10 for a range of speed from 900 to 1400 feet per second. The peak pressure ratio and maximum adiabatic efficiency at 1300-feet-per-second equivalent speed were 3.15



and 0.805, respectively. At the maximum speed of 1400 feet per second, the peak pressure ratio was 3.58 and the maximum efficiency was 0.785. The average Mach number at the outlet measuring station for the maximum-efficiency points over the range of speed was between 0.37 and 0.46.

## DISCUSSION OF RESULTS

The purpose of this report is to determine the reliability of the design technique as applied to the three centrifugal impellers used for this investigation. The design technique consists in using the design method of reference 4 and of specifying the velocity so that the eddy and decelerating flow are avoided insofar as possible. In order to determine whether the use of the design technique results in significant improvement in performance, it is necessary to compare the performance of the modified and original impellers.

### Comparison of Original and Modified Parabolic-Bladed Impellers

The performance of the original and modified parabolic-bladed impellers is discussed in reference 5. Some of that discussion is repeated herein. The performance of the modified parabolic-bladed impeller with vaneless diffuser shows considerable improvement over that of the original impeller (fig. 11(a)). This improvement may be explained by a study of the internal-flow characteristics of each impeller. An analysis of the flow in the blade-to-blade plane of the original impeller (1331-ft/sec impeller equivalent speed) showed a large eddy on the driving face of the blade at the hub (fig. 3(a)). (Eddy formation is taken herein as beginning when the theoretical velocity on the blade surface becomes negative.) If the reversal of flow that accompanies the formation of the eddy is experimentally unstable, separation and rotating stall such as discussed in reference 3 may occur. If the rotating stall does not result in surge or results in surge mild enough to allow operation at a lower weight flow, a second stall or surge point caused by too large a relative inlet angle will be reached. Two surge points for some operating speeds are shown in figure 4 of reference 3. This phenomenon may be the result of such an occurrence. For the original parabolic-bladed impeller, the unstable eddy apparently caused violent surge at 1400 and 1500 feet per second (fig. 11(a)), whereas at lower speeds it merely caused a reduction in efficiency with decreasing weight flow.

In redesigning the original impeller, the tendency toward eddy formation was decreased by increasing the theoretical velocity ratio (ratio of velocity relative to impeller to stagnation speed of sound upstream of impeller inlet) from 0.17 to 0.55 (fig. 1(a)) in the region where the eddy occurred near the outlet (fig. 3(a)). Thus, the increased performance of the modified over the original impeller results from a combination

of reduced velocity gradients and the decrease of the tendency toward eddy formation, which enables the modified impeller to operate successfully at high speeds.

The difference in pressure ratio of the modified and original impellers (fig. 11(a)) is small at 900 and 1100 feet per second, but the difference in efficiency is large (0.05 to 0.07). This may be accounted for by the poor internal-flow characteristics of the original impeller. The reversal of flow accompanying the eddy in the original impeller may cause particles of air inside the impeller that have had whirl imparted to them to flow upstream (backflow) into the inlet section ahead of the impeller. These particles of air then re-enter the impeller at a higher temperature than if there had been no backflow. Thus, the large difference in efficiencies between the two impellers at low speeds may be attributed in part to the low efficiency of the original impeller caused by an increased outlet temperature due to backflows at the impeller inlet. This backflow phenomenon also contributes to the decreasing efficiency of the modified impeller at 900 feet per second at weight flows less than 4.75 pounds per second (fig. 8(b)), with the point at 2.05 pounds per second probably in mild surge (inaudible). In violent surge (audible), the backflow phenomenon could be detected by an increase in the inlet temperature in the surge tank approximately 7 impeller diameters upstream of the impeller inlet. A study of the backflow phenomenon is presented in reference 13.

#### Comparison of Original and Modified Circular-Bladed Impellers

The modified circular-bladed impeller had higher pressure ratios and efficiencies than the original circular-bladed impeller at all speeds investigated, with the greatest gain in performance occurring at the higher speeds (fig. 11(b)). At a speed of 1400 feet per second, the modified impeller was 0.127 higher in efficiency than the original impeller. It is possible that eddy formation in the original impeller began at a speed of 1200 feet per second, as indicated by the unusual curve for that speed in figure 11(b). At speeds of 1400 and 1500 feet per second for the original impeller, it is probable that the eddy caused unstable operating characteristics (ref. 1) and finally premature surge. The modified impeller also evidenced eddy formation at speeds of 1400 and 1500 feet per second, where premature surge occurred. However, as the theoretical design for this impeller was further away from the condition necessary for eddy formation than was the original impeller, higher pressure ratios and efficiencies were obtained at the higher speeds for the modified impeller.

It is probable that the premature surge of the modified impeller at high speeds could be avoided by changing the hub contour or blade thickness. This would result in increased performance for the modified impeller at these speeds.

### Comparison of Original and Modified Skewed-Parabolic-Bladed Impellers

The modified skewed-parabolic-bladed impeller had better performance than the original skewed-parabolic-bladed impeller at all speeds investigated, with the greatest gains being made at speeds above 1200 feet per second (fig. 11(c)). Eddy formation in the original impeller probably began at a speed of 900 feet per second, as shown by the dropping off (lowering) of the pressure ratio at weight flows less than 5.75 pounds per second. The results of eddy formation become more severe at speeds above 900 feet per second, causing erratic pressure ratios and a rapid lowering of the efficiency at speeds above 1200 feet per second. It is probable that eddy formation in the original impeller would have caused premature surge at speeds above 1300 feet per second.

The performance results for the modified skewed-parabolic-bladed impeller (fig. 11(c)) indicate that this impeller did not evidence eddy formation at the speeds investigated. However, the theoretical blade-loading diagrams of figure 5 indicate that the velocity on the driving face of the blade near the hub approaches zero and is thus near the theoretical condition necessary for eddy formation.

### Comparison of Modified Parabolic-, Circular-, and Skewed-Parabolic-Bladed Impellers

The pressure ratios of the three modified impellers are within 6 percent of each other at all speeds investigated, as shown in figure 12. The pressure ratios for the two parabolic-bladed impellers were nearly the same at all speeds investigated. The circular-bladed impeller had slightly higher pressure ratios than the parabolic-bladed impellers at speeds up to 1200 feet per second and slightly lower pressure ratios at speeds above 1300 feet per second.

The power input required to achieve these pressure ratios varied greatly for the three impellers, as is shown by the curves for maximum adiabatic efficiency in figure 12. The parabolic-bladed impeller had the highest efficiencies at all speeds investigated, and the skewed-parabolic-bladed impeller was 0.015 to 0.040 less efficient than the parabolic-bladed impeller. The circular-bladed impeller was 0.01 less efficient than the parabolic-bladed impeller at 900 feet per second, the difference in efficiency increasing with increasing speed to 0.142 at 1500 feet per second.

The weight-flow range for the three impellers is also shown in figure 12. The parabolic- and skewed-parabolic-bladed impellers had approximately the same weight-flow range at speeds up to 1300 feet per second. At speeds of 1400 and 1500 feet per second, the parabolic-bladed impeller

had much greater range than the other two impellers. The very small weight-flow range of the circular-bladed impeller at speeds of 1400 and 1500 feet per second was possibly due to premature surge associated with the presence of an eddy in the potential-flow solution. Premature surge may be defined as surge due to conditions other than exceeding the stalling angle of attack. This premature surge also accounts for the low efficiency of the circular-bladed impeller at these speeds. The theoretical blade-loading diagrams (figs. 3 to 5) indicate that the circular- and skewed-parabolic-bladed impellers more nearly approach the theoretical condition for eddy formation (negative velocity ratio on driving face of blade) than does the parabolic-bladed impeller. The parabolic-bladed impeller was best designed of the three impellers with respect to elimination of the tendency for eddy formation and flow decelerations along the hub. This may account for the better weight-flow range and efficiency of this impeller, especially at speeds of 1300 feet per second and higher.

Some degree of comparison of blade shapes may be made between the skewed-parabolic-bladed impeller and the circular-bladed impeller, inasmuch as these two impellers had the same velocity distributions along the hub (figs. 1(b) and (c)), the same weight flows through the impellers, and the same blade height at the inlet. Their hub and shroud shapes, as well as their blade shapes, were different. A comparison of the blade-to-blade velocity distributions (figs. 4 and 5) shows that the circular-bladed impeller is more highly loaded in the inlet section than is the skewed-parabolic-bladed impeller. The higher loading at inlet for the circular-bladed impeller is probably the result of a larger angle of attack for this weight flow than for the skewed-parabolic-bladed impeller. This is also reflected in the surge lines (fig. 12) for the speeds where surge is attributed to angle of attack at the inlet. The circular-bladed impeller surges at a higher weight flow than the skewed-parabolic-bladed impeller.

On the basis of the over-all data (figs. 9 and 10), it appears that the skewed-parabolic blading is more desirable than the circular blading. However, more investigation would be necessary to determine whether this is the case. At design, both of these impellers were operating near the eddy condition. Why the circular-bladed impeller evidenced premature surge at speeds above 1300 feet per second and the skewed-parabolic-bladed impeller did not is difficult to explain. It may be that the assumption of radial blade elements and other approximations in the design method masked small differences in the two shapes and that the arbitrary boundary-layer allowance magnified these differences. Also, the lighter blade loading at the inlet of the skewed-parabolic-bladed impeller may have contributed to the better operating characteristics of this impeller. At any rate, in the design of a new impeller, operation so near the eddy condition probably should not be allowed.

## SUMMARY OF RESULTS

Three centrifugal impellers were modified by assigning a new velocity distribution that reduced the velocity gradients from inlet to outlet along the hub and applying the design procedure of NACA TN 3399 to arrive at a new shroud contour. An investigation of the performance characteristics of the modified impellers produced the following results:

1. The modified impellers, as compared with the original impellers, had higher peak pressure ratios and maximum efficiencies at all speeds investigated, with the greatest gains at speeds of 1300 feet per second and higher.
2. The large gains in performance of the modified impellers compared with the original impellers at speeds of 1300 feet per second and higher probably resulted primarily from more favorable velocity gradients and from designing these impellers further away from the condition necessary for eddy formation. The modified impellers were thus able to operate over a wider range of weight flows at high speeds.
3. The experimental results indicate that the design method of NACA TN 3399 is a reliable method for designing centrifugal compressors, since significant increases in performance were achieved by applying the design method to three centrifugal impellers.
4. The peak pressure ratio and maximum adiabatic efficiency based on measurements taken at a radius twice the impeller radius in a vaneless diffuser for the three modified impellers at 1300-feet-per-second equivalent speed (design speed, 1331 ft/sec) were as follows: parabolic-bladed impeller, 3.07 and 0.825; circular-bladed impeller, 3.13 and 0.737; skewed-parabolic-bladed impeller, 3.15 and 0.805. Of the three modified impellers, the parabolic-bladed impeller had the highest maximum efficiencies (0.854 to 0.800) and the best weight-flow range over the speed range tested.
5. On the basis of the theoretical and experimental results, it appears that the blading of the parabolic-bladed impellers is more desirable than that of the circular-bladed impeller. However, more investigation is necessary to determine whether this is the case.

Lewis Flight Propulsion Laboratory  
National Advisory Committee for Aeronautics  
Cleveland, Ohio, December 7, 1956

## REFERENCES

1. Anderson, Robert J., Ritter, William K., and Dildine, Dean M.: An Investigation of the Effect of Blade Curvature on Centrifugal-Impeller Performance. NACA TN 1313, 1947.
2. Hamrick, Joseph T., Ginsburg, Ambrose, and Osborn, Walter M.: Method of Analysis for Compressible Flow Through Mixed-Flow Centrifugal Impellers of Arbitrary Design. NACA Rep. 1082, 1952. (Supersedes NACA TN 2165.)
3. Emmons, H. W., Pearson, C. E., and Grant, H. P.: Compressor Surge and Stall Propagation. Trans. A.S.M.E., vol. 77, no. 4, May 1955, pp. 455-467; discussion, pp. 467-469.
4. Smith, Kenneth J., and Hamrick, Joseph T.: A Rapid Approximate Method for the Design of Hub Shroud Profiles of Centrifugal Impellers of Given Blade Shape. NACA TN 3399, 1955.
5. Smith, Kenneth J., and Osborn, Walter M.: Design and Test of Mixed-Flow Impellers. VI - Performance of Parabolic-Bladed Impeller with Shroud Redesigned by Rapid Approximate Method. NACA RM E55F23, 1955.
6. Osborn, Walter M., and Hamrick, Joseph T.: Design and Test of Mixed-Flow Impellers. I - Aerodynamic Design Procedure. NACA RM E52E05, 1952.
7. Withee, Joseph R., Jr., and Beede, William L.: Design and Test of Mixed-Flow Impellers. II - Experimental Results, Impeller Model MFI-1A. NACA RM E52E22, 1952.
8. Hamrick, Joseph T., Osborn, Walter M., and Beede, William L.: Design and Test of Mixed-Flow Impellers. III - Design and Experimental Results for Impeller Model MFI-2A and Comparison with Impeller Model MFI-1A. NACA RM E52L22a, 1953.
9. Hamrick, Joseph T., Beede, William L., and Withee, Joseph R., Jr.: Design and Test of Mixed-Flow Impellers. IV - Experimental Results for Impeller Models MFI-1 and MFI-2 with Changes in Blade Height. NACA RM E53L02, 1954.
10. Hamrick, Joseph T., and Osborn, Walter M.: Design and Test of Mixed-Flow Impellers. V - Design Procedure and Performance Results for Two Vaned Diffusers Tested with Impeller Model MFI-1B. NACA RM E55E13, 1955.

11. Osborn, Walter M.: Design and Test of Mixed-Flow Impellers. VII - Experimental Results for Parabolic-Bladed Impeller with Alternate Blades Cut Back to Form Splitter Vanes. NACA RM E55L15, 1956.
12. Osborn, Walter M.: Performance of Mixed-Flow Impeller, Model MFI-1B, with Diffuser Vanes at Equivalent Impeller Speeds from 1100 to 1700 Feet Per Second. NACA RM E54D23, 1954.
13. Benser, William A., and Moses, Jason J.: An Investigation of Back-flow Phenomenon in Centrifugal Compressors. NACA Rep. 806, 1945. (Supersedes NACA WR E-8.)

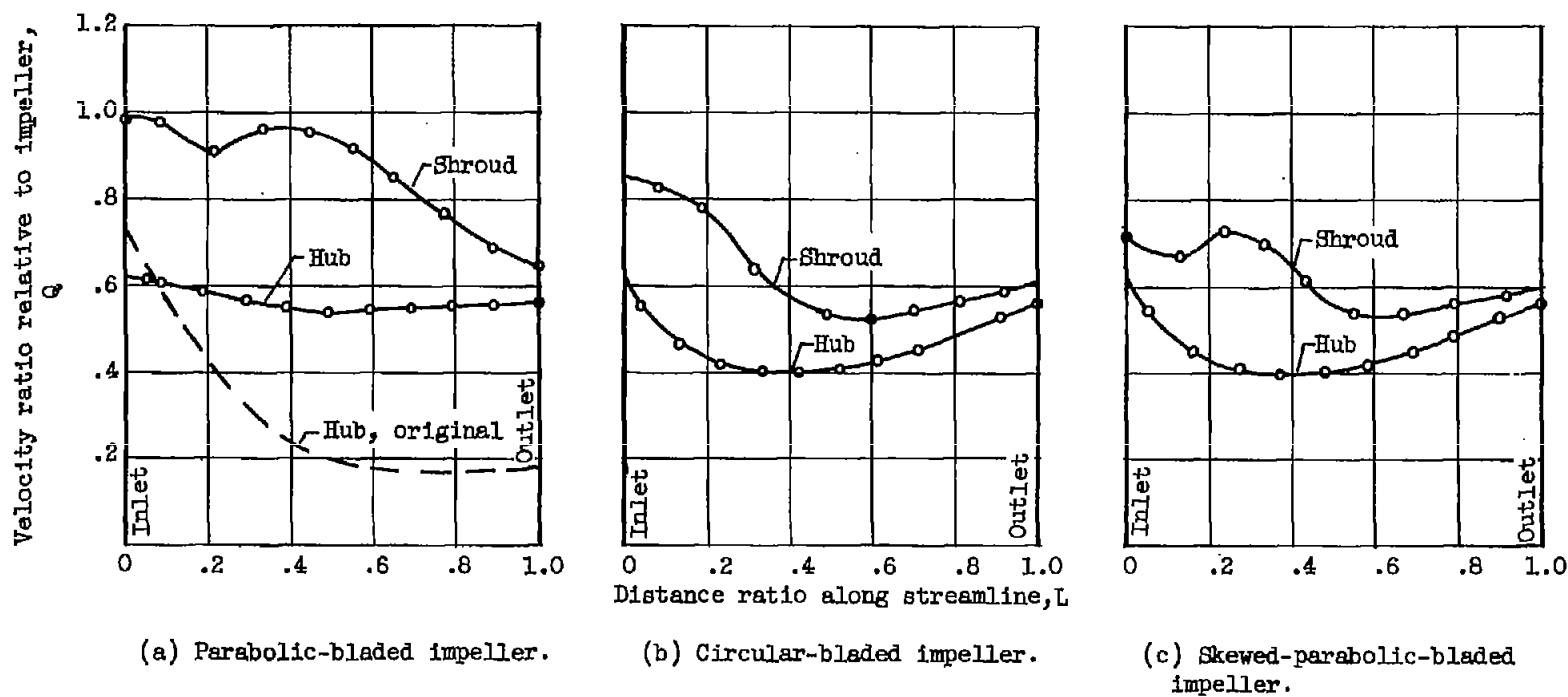


Figure 1. - Comparison of hub and shroud velocities for redesigned (isentropic) parabolic-, circular-, and skewed-parabolic-bladed impellers.



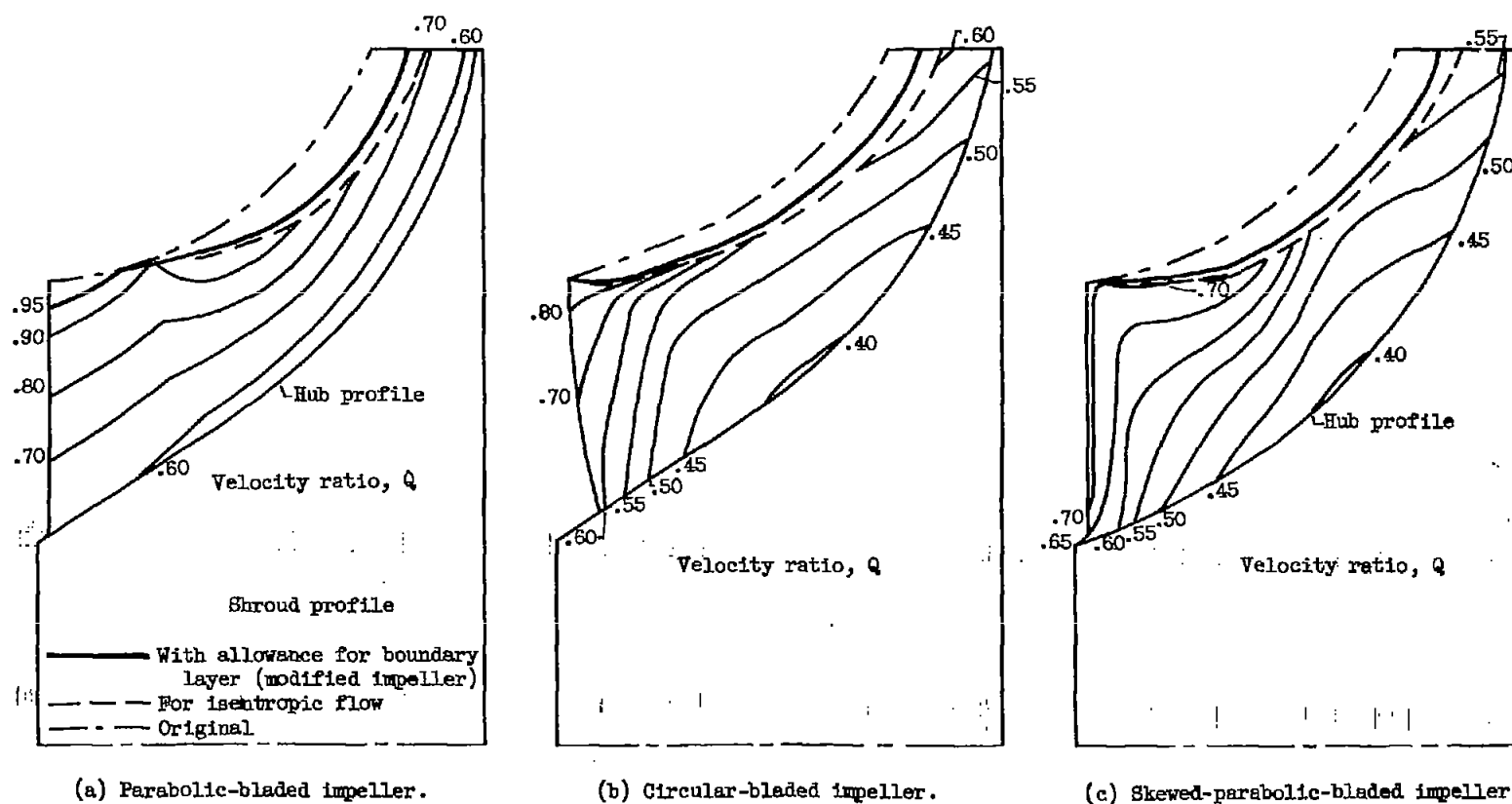


Figure 2. - Comparison of hub-shroud profiles of original, modified, and isentropic designs for parabolic-, circular-, and skewed-parabolic-bladed impellers. Contours of velocity ratio in hub-shroud plane for isentropic design are also shown.

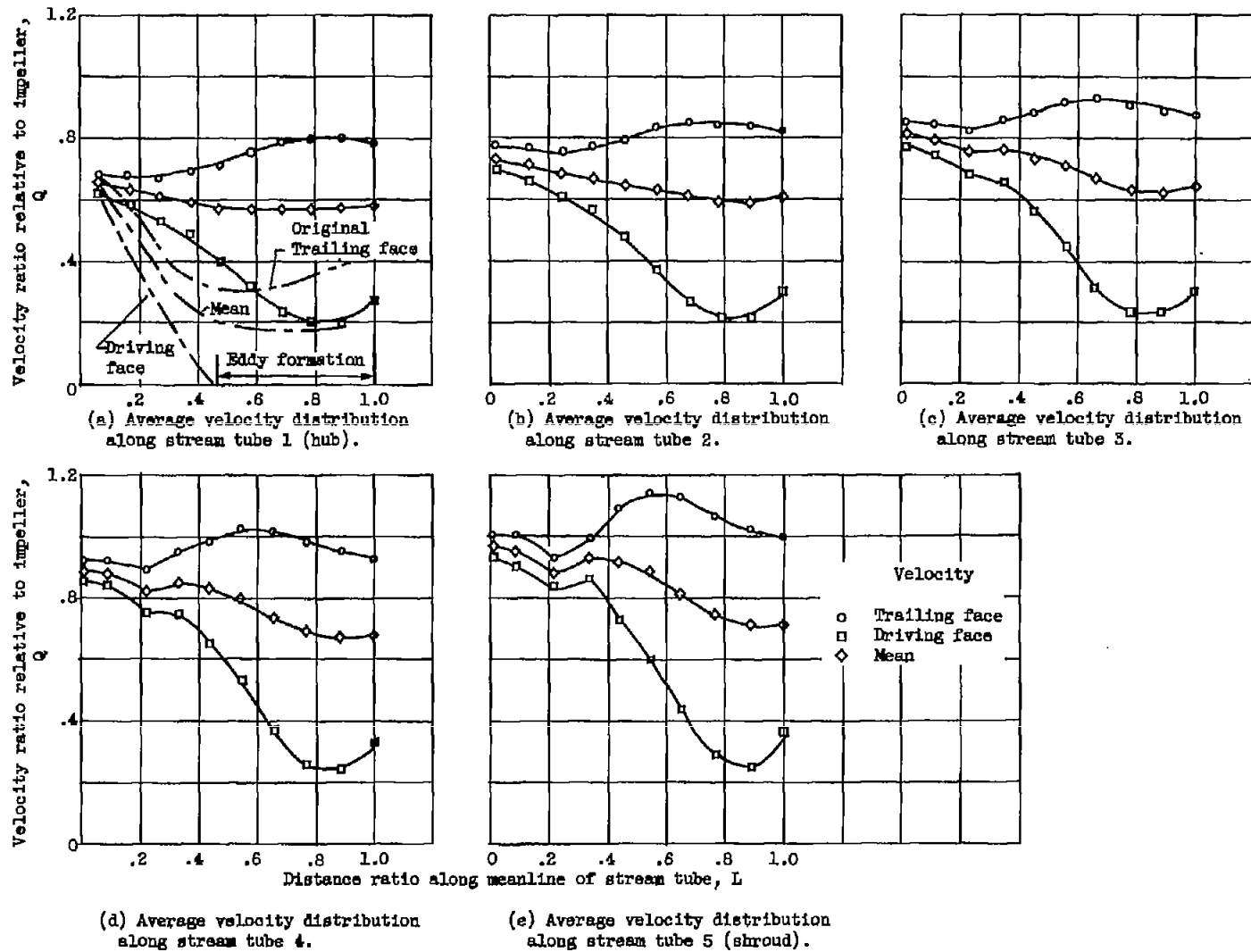


Figure 3. - Blade-to-blade velocity distribution for redesigned (isentropic) parabolic-bladed impeller at meanline of hub-shroud stream tube for weight flow of 8.38 pounds per second and outlet speed of 1331 feet per second (five stream tubes used for design).

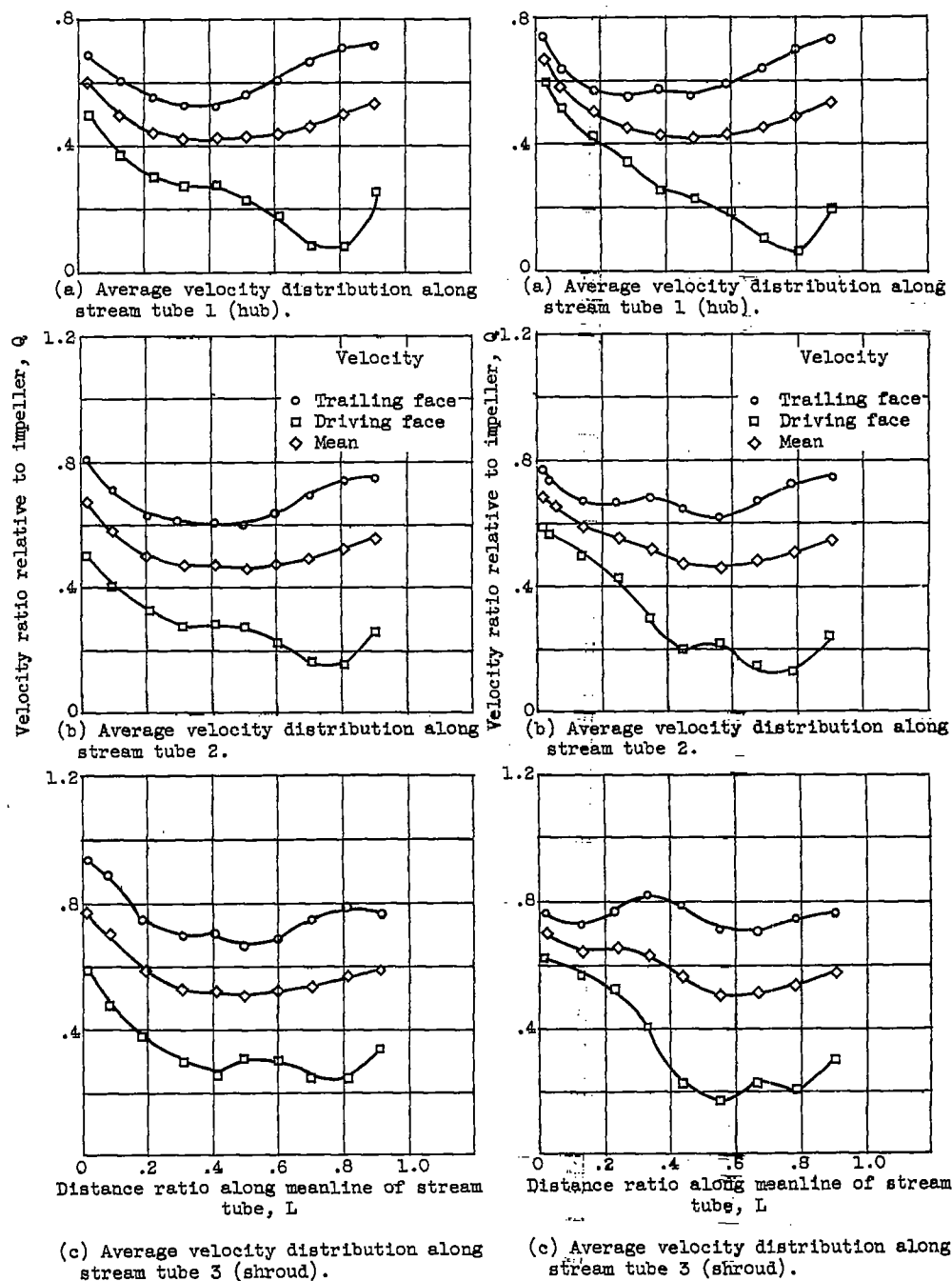
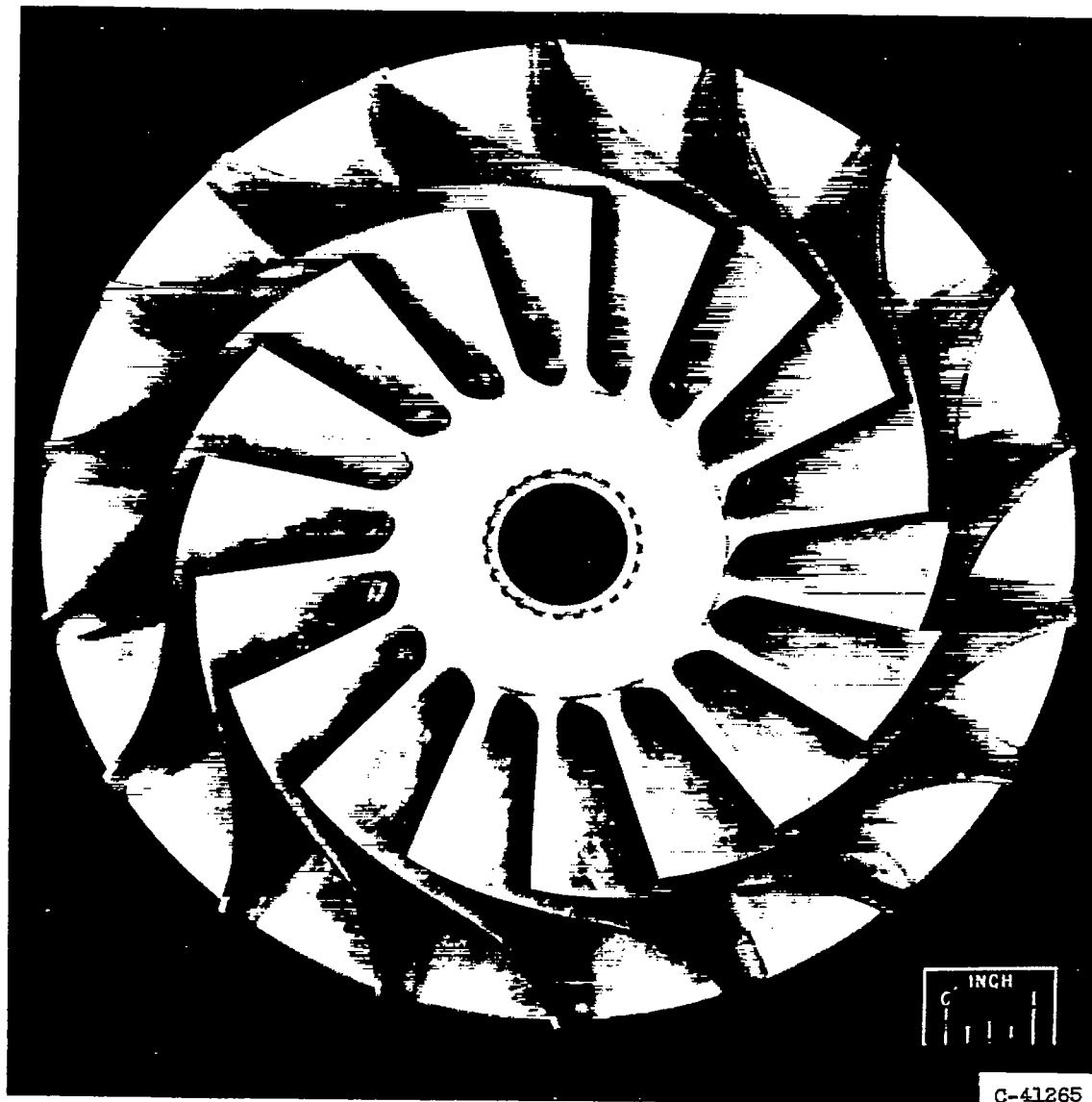


Figure 4. - Blade-to-blade velocity distribution for redesigned (isentropic) circular-bladed impeller at meanline of hub-shroud stream tube for weight flow of 8.16 pounds per second and outlet speed of 1331 feet per second (three stream tubes used for design).

Figure 5. - Blade-to-blade velocity distribution for redesigned (isentropic) skewed-parabolic-bladed impeller at meanline of hub-shroud stream tube for weight flow of 8.0 pounds per second and outlet speed of 1331 feet per second (three stream tubes used for design).

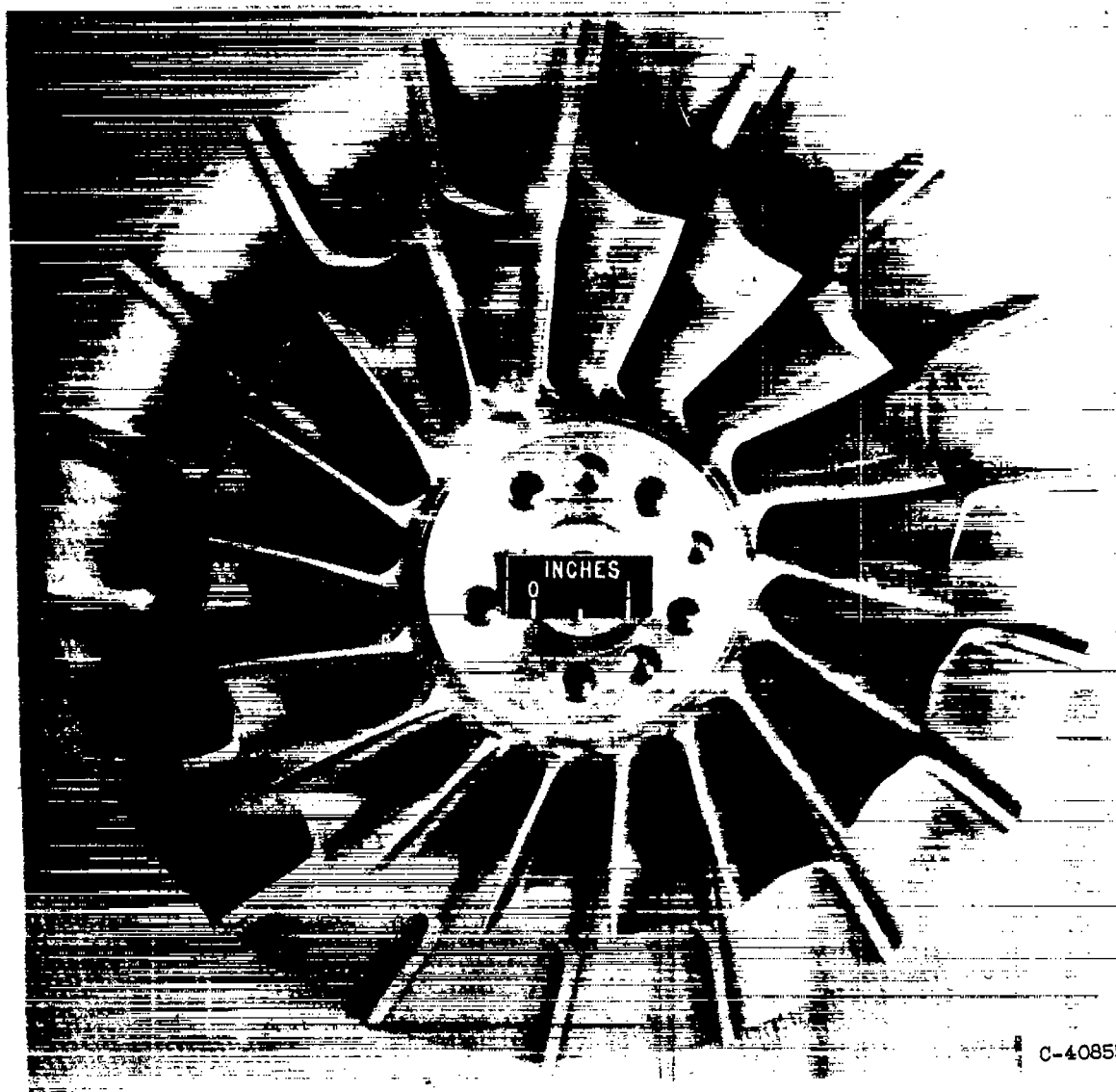


(a) Parabolic-bladed impeller.

Figure 6. - Modified impellers.

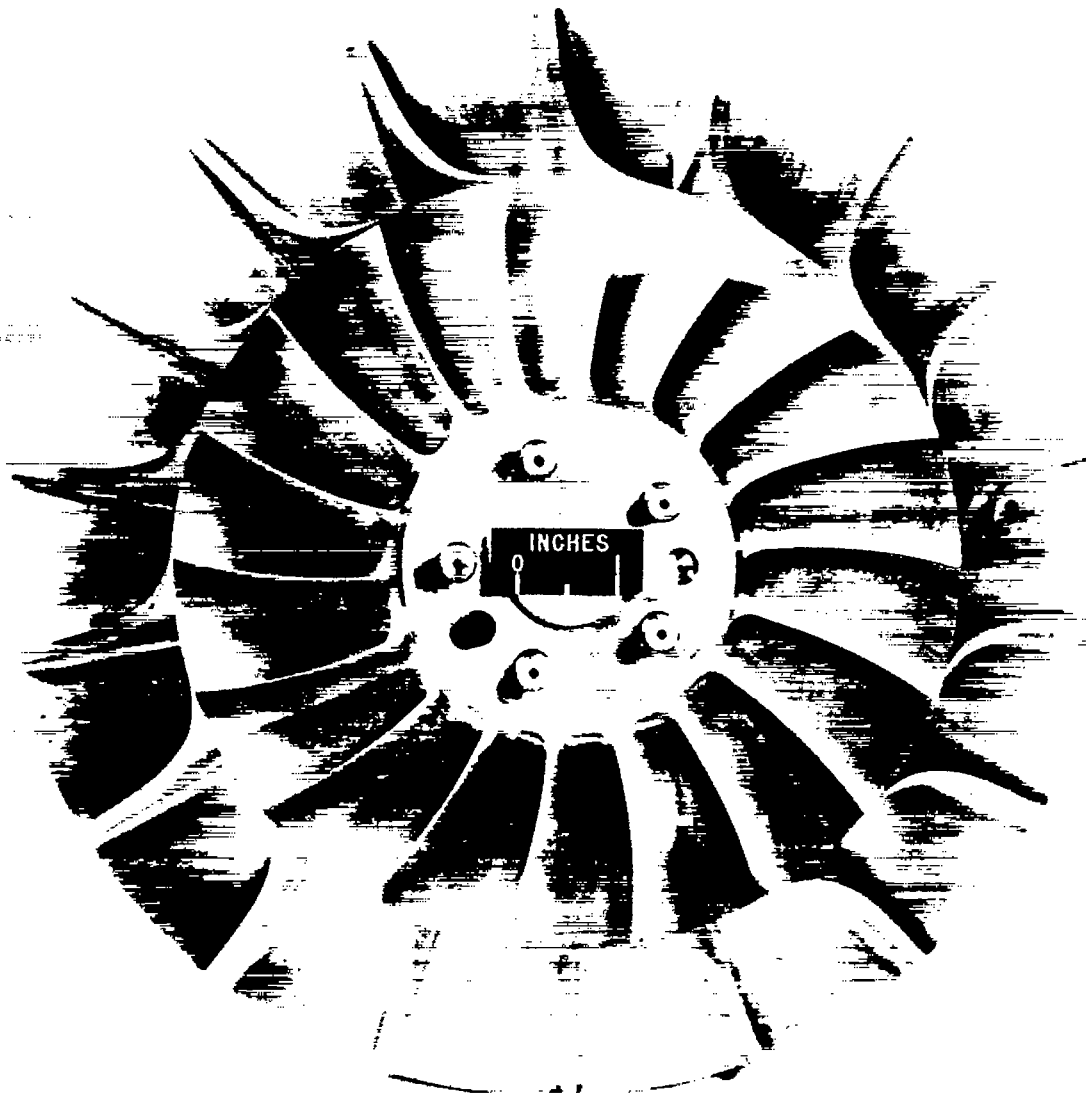
4243

CTI-3 back



(b) Circular-bladed impeller.

Figure 6. - Continued. Modified impellers.



C-40856

(c) Skewed-parabolic-bladed impeller.

Figure 6. - Concluded. Modified impellers.

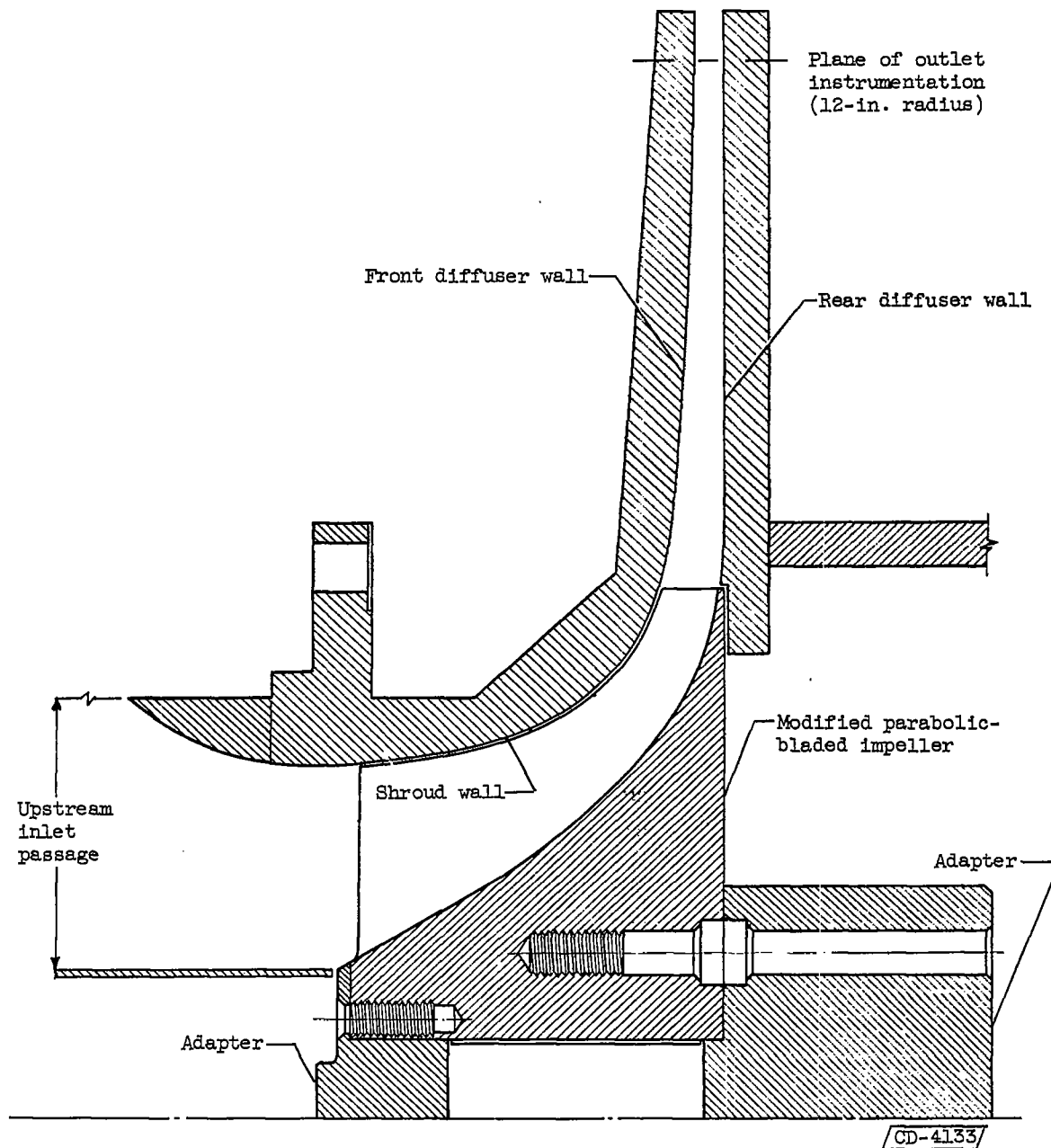
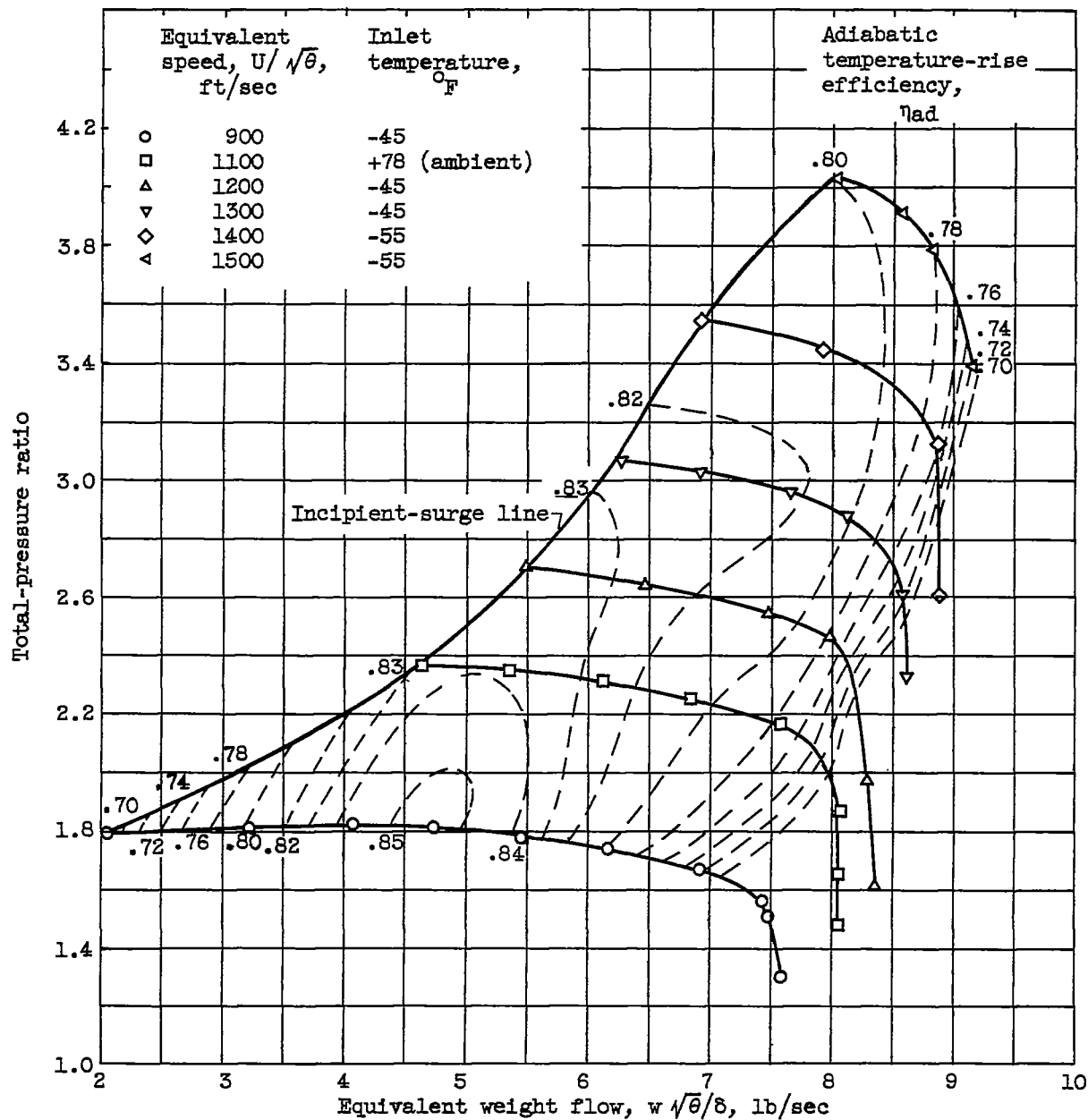


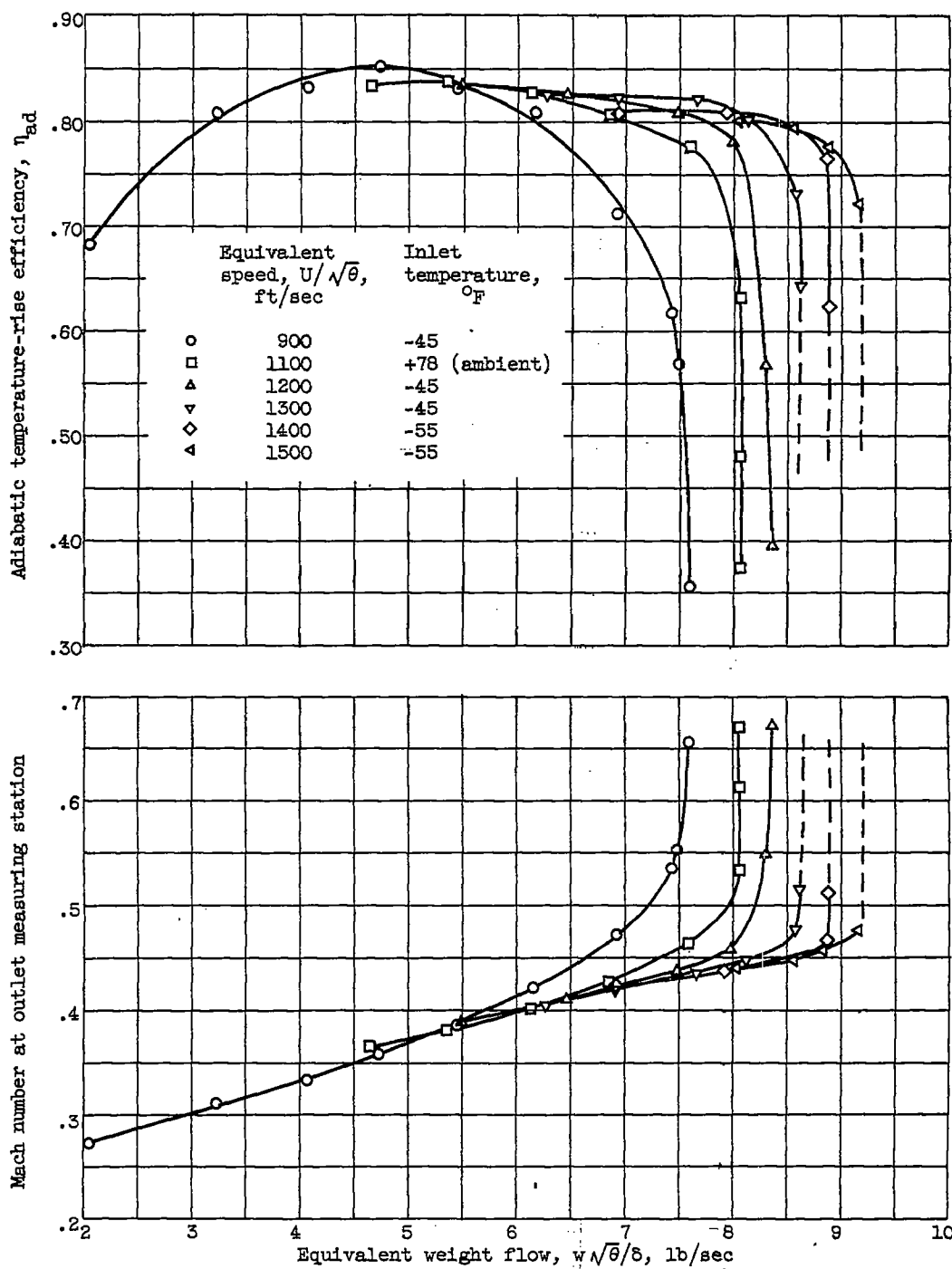
Figure 7. - Cross-sectional view of modified parabolic-bladed impeller and diffuser showing location of outlet instrumentation.



(a) Performance characteristics.

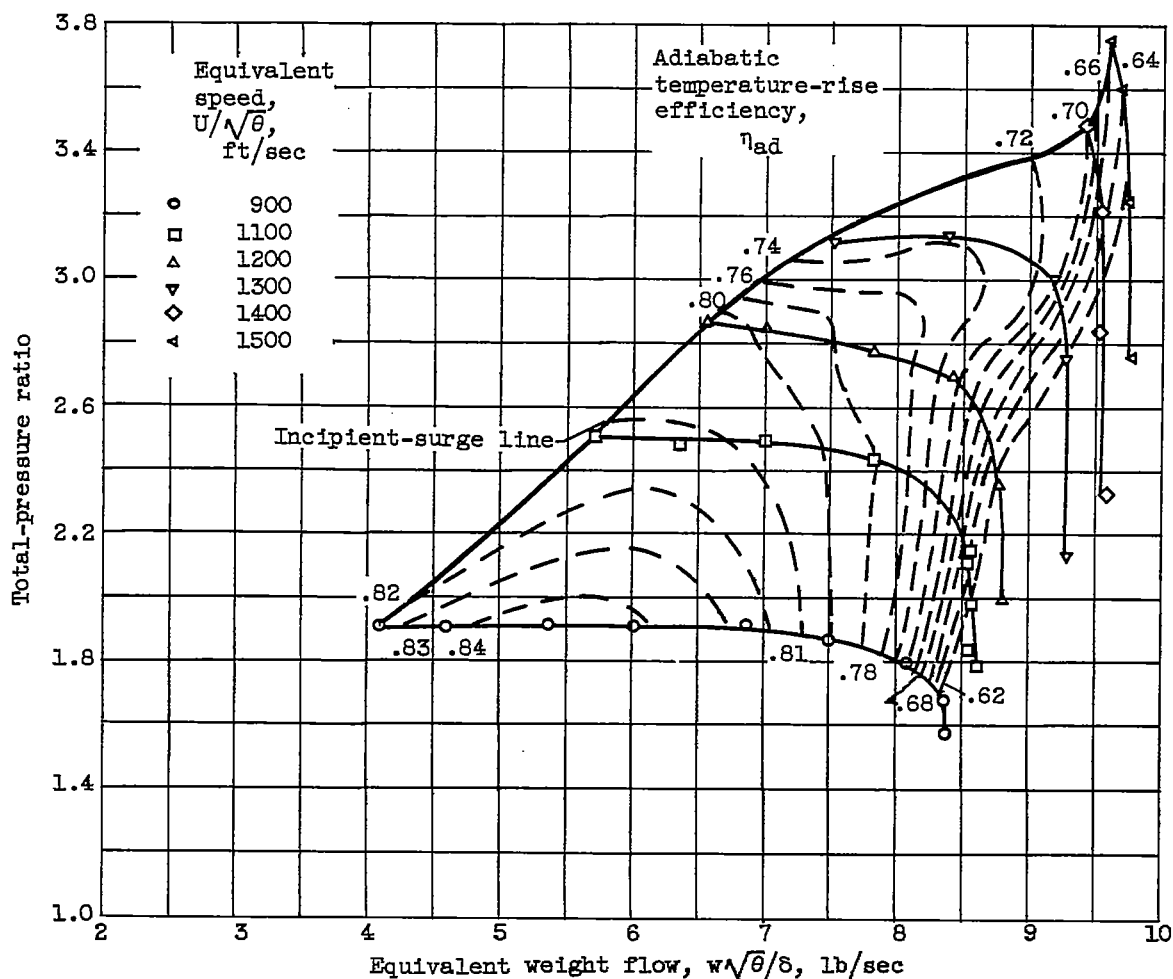
Figure 8. - Over-all performance characteristics of modified parabolic-bladed impeller with vaneless diffuser at inlet-air pressure of 20 inches of mercury absolute.





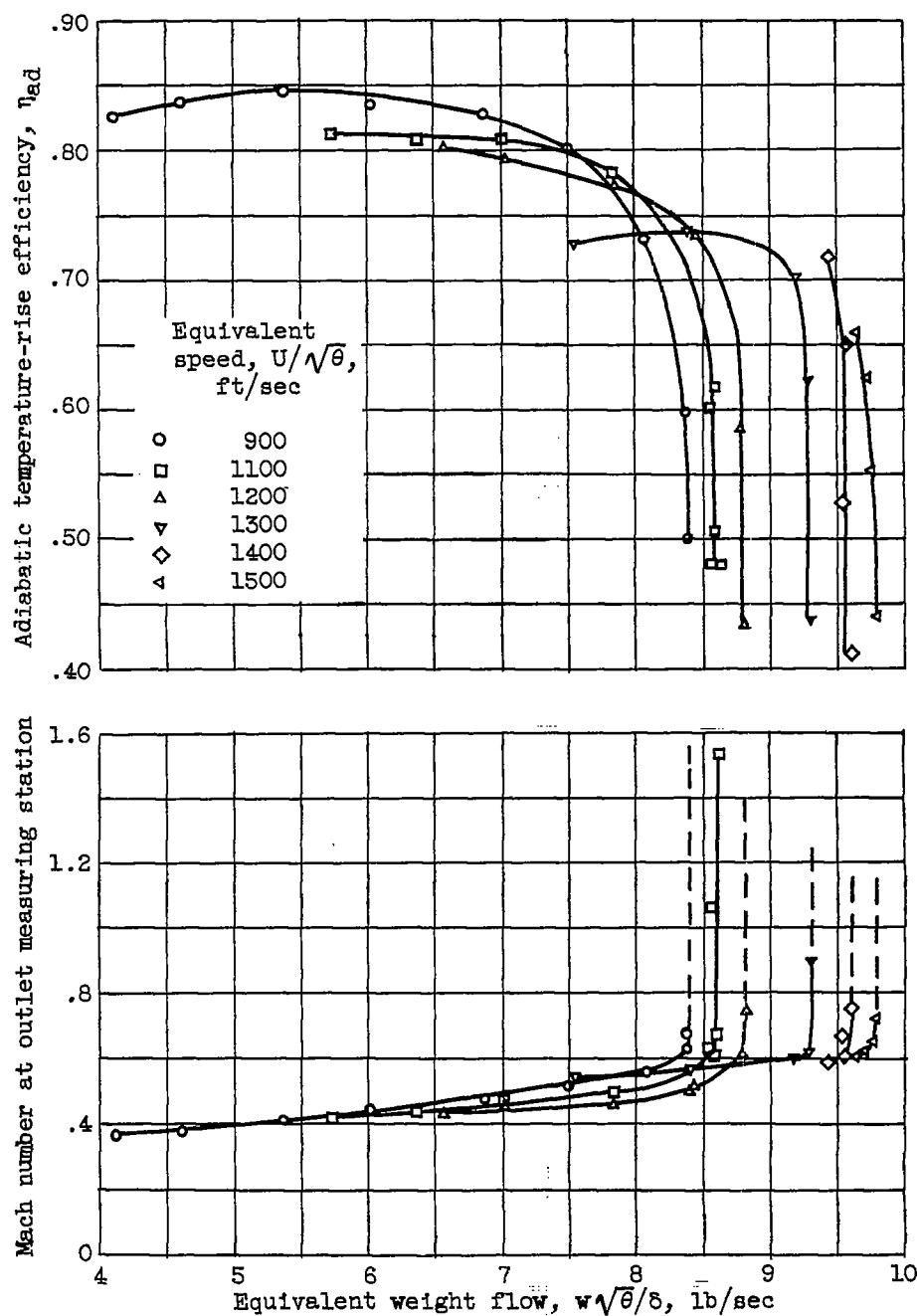
(b) Efficiency and Mach number.

Figure 8. - Concluded. Over-all performance characteristics of modified parabolic-bladed impeller with vaneless diffuser at inlet-air pressure of 20 inches of mercury absolute.



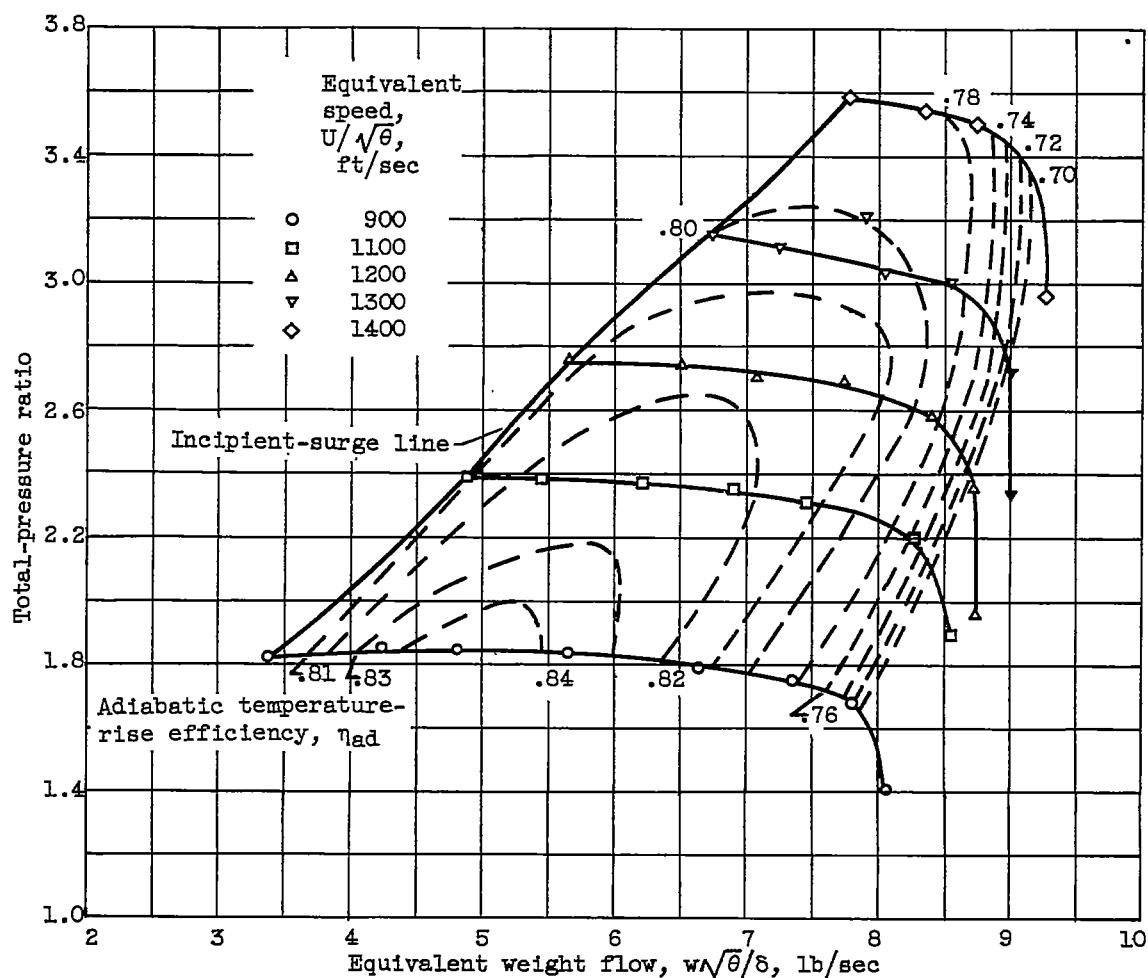
(a) Performance characteristics.

Figure 9. - Over-all performance characteristics of modified circular-bladed impeller with vaneless diffuser at inlet-air pressure of 20 inches of mercury absolute. Inlet temperature,  $-50^{\circ}\text{F}$ .



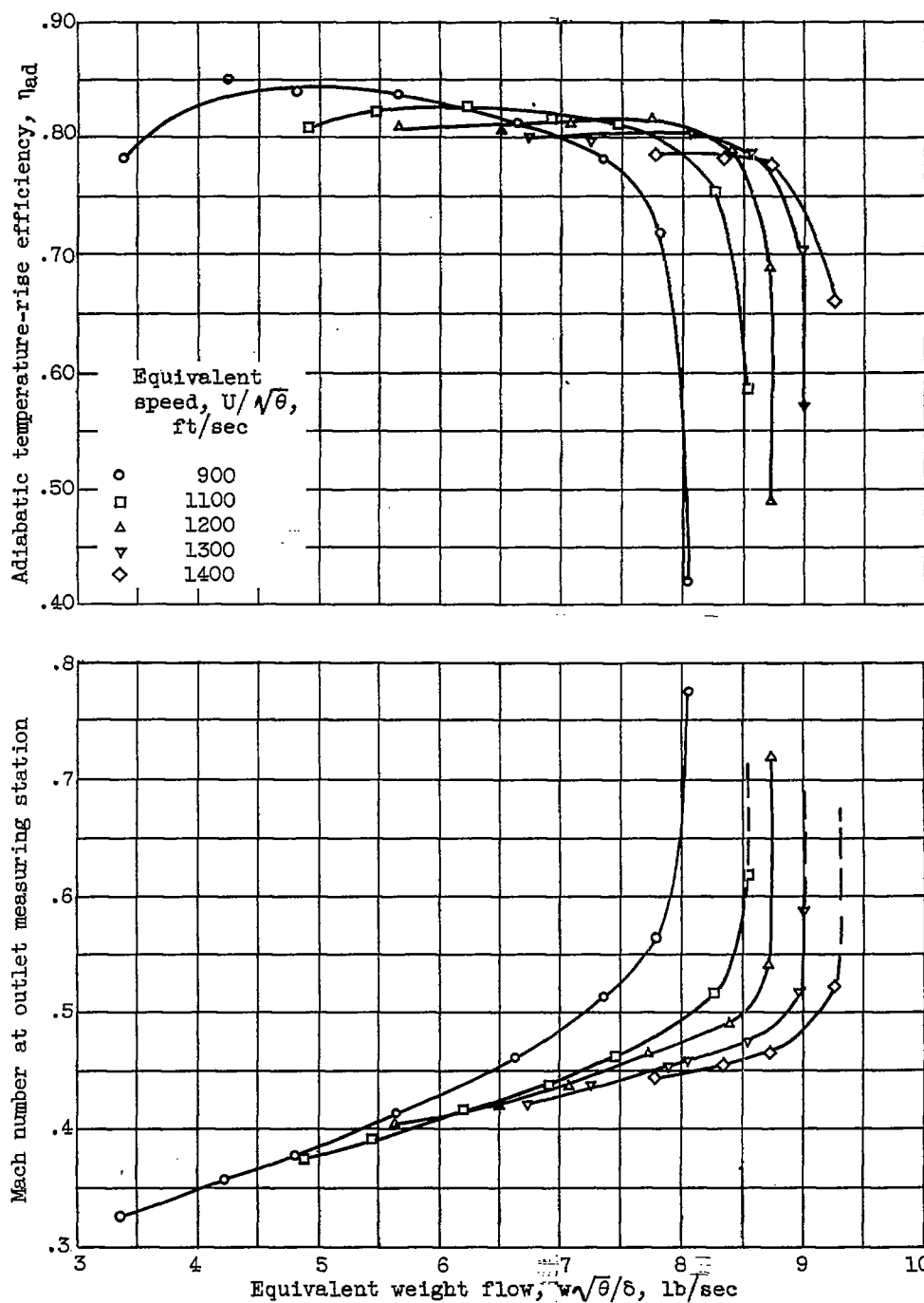
(b) Efficiency and Mach number.

Figure 9. - Concluded. Over-all performance characteristics of modified circular-bladed impeller with vaneless diffuser at inlet-air pressure of 20 inches of mercury absolute. Inlet temperature,  $-50^{\circ}$  F.



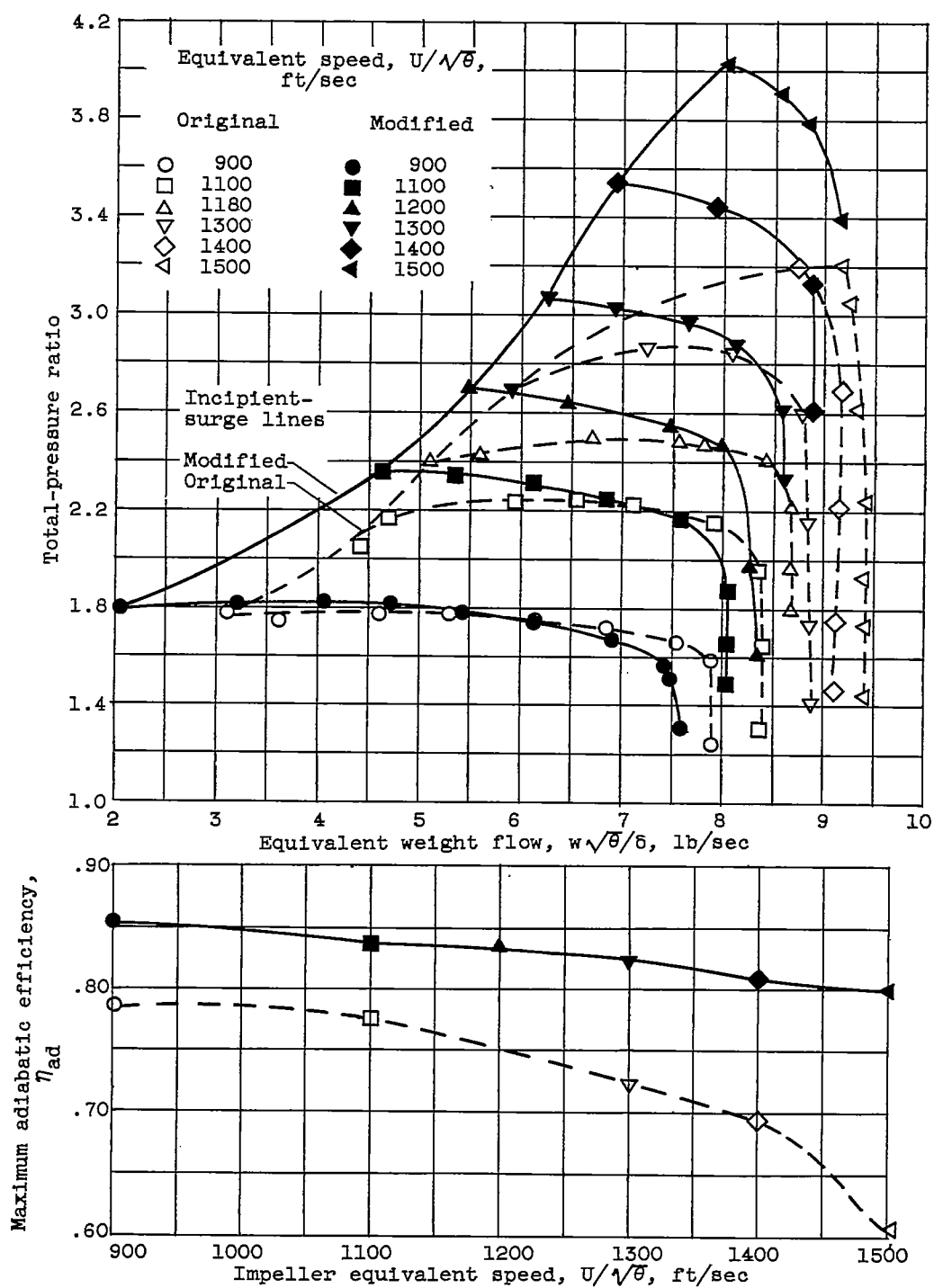
(a) Performance characteristics.

Figure 10. - Over-all performance characteristics of modified skewed-parabolic-bladed impeller with vaneless diffuser at inlet-air pressure of 20 inches of mercury absolute. Inlet temperature,  $-45^{\circ}\text{F}$ .



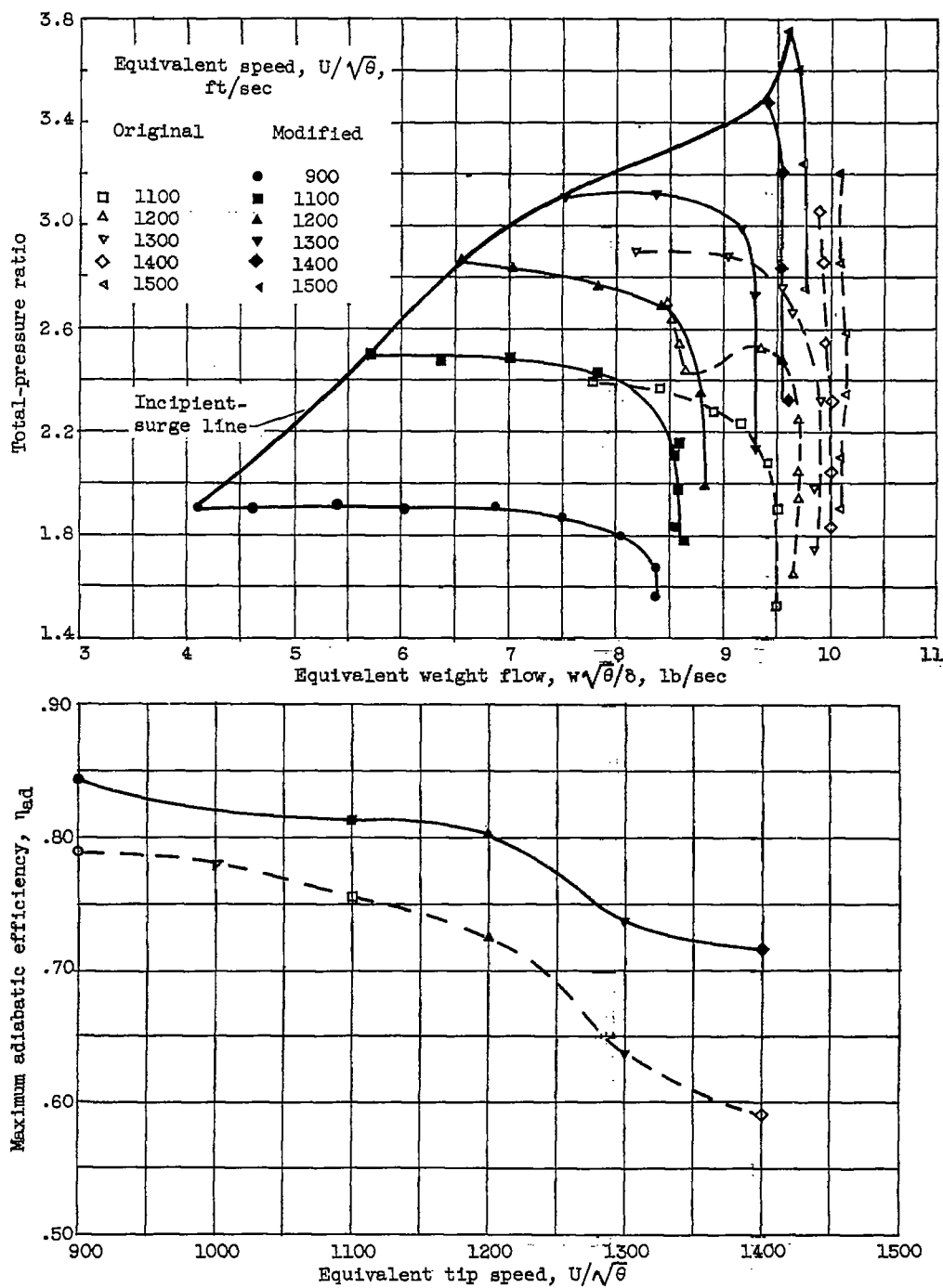
(b) Efficiency and Mach number.

Figure 10. - Concluded. Over-all performance characteristics of modified skewed-parabolic-bladed impeller with vaneless diffuser, at inlet-air pressure of 20 inches of mercury absolute. Inlet temperature,  $-45^{\circ}$  F.



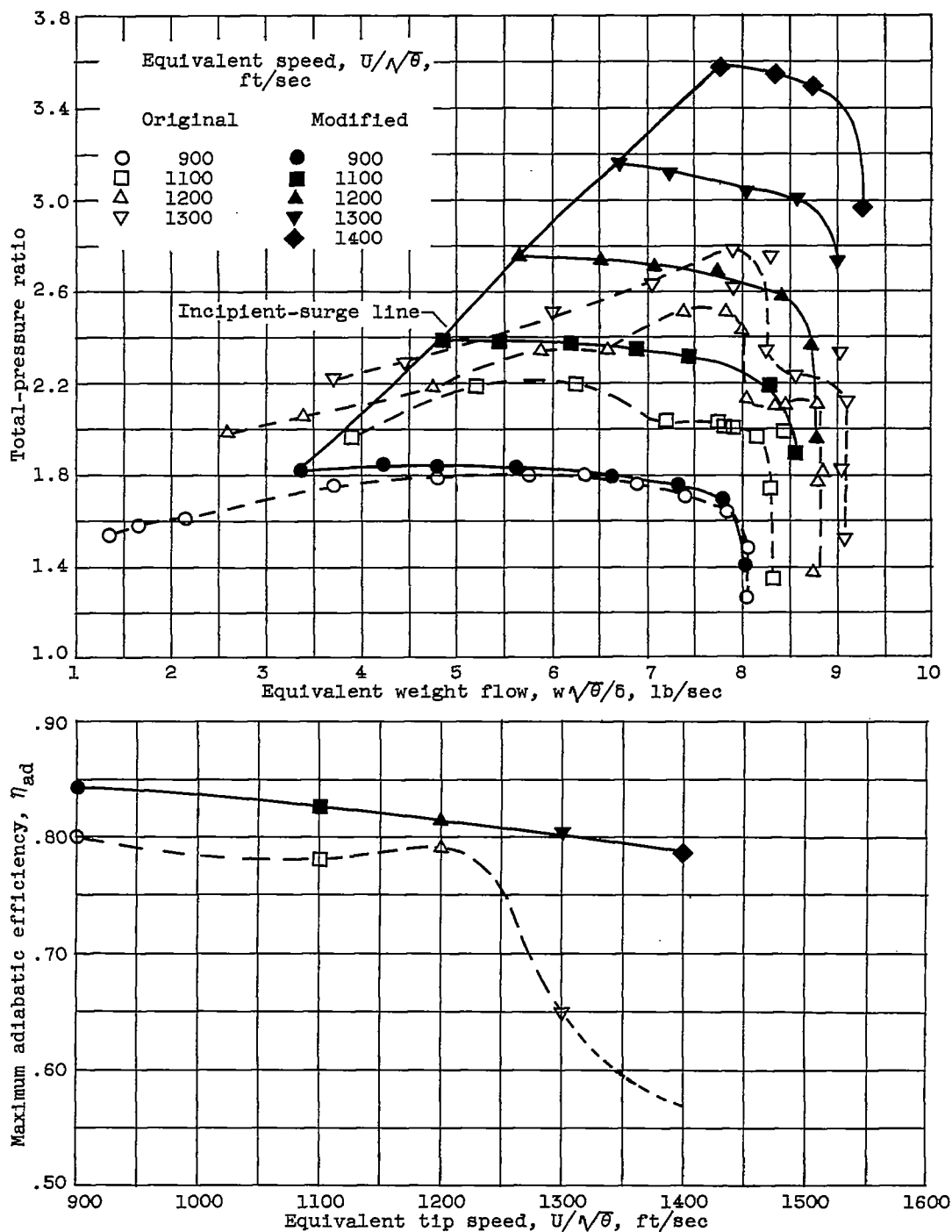
(a) Parabolic-bladed impellers.

Figure 11. - Comparison of performance of modified and original parabolic-, circular-, and skewed-parabolic-bladed impellers with vaneless diffuser.



(b) Circular-bladed impellers.

Figure 11. - Continued. Comparison of performance of modified and original parabolic-, circular-, and skewed-parabolic-bladed impellers with vaneless diffuser.



(c) Skewed-parabolic-bladed impellers.

Figure 11. - Concluded. Comparison of performance of modified and original parabolic-, circular-, and skewed-parabolic-bladed impellers with vaneless diffuser.



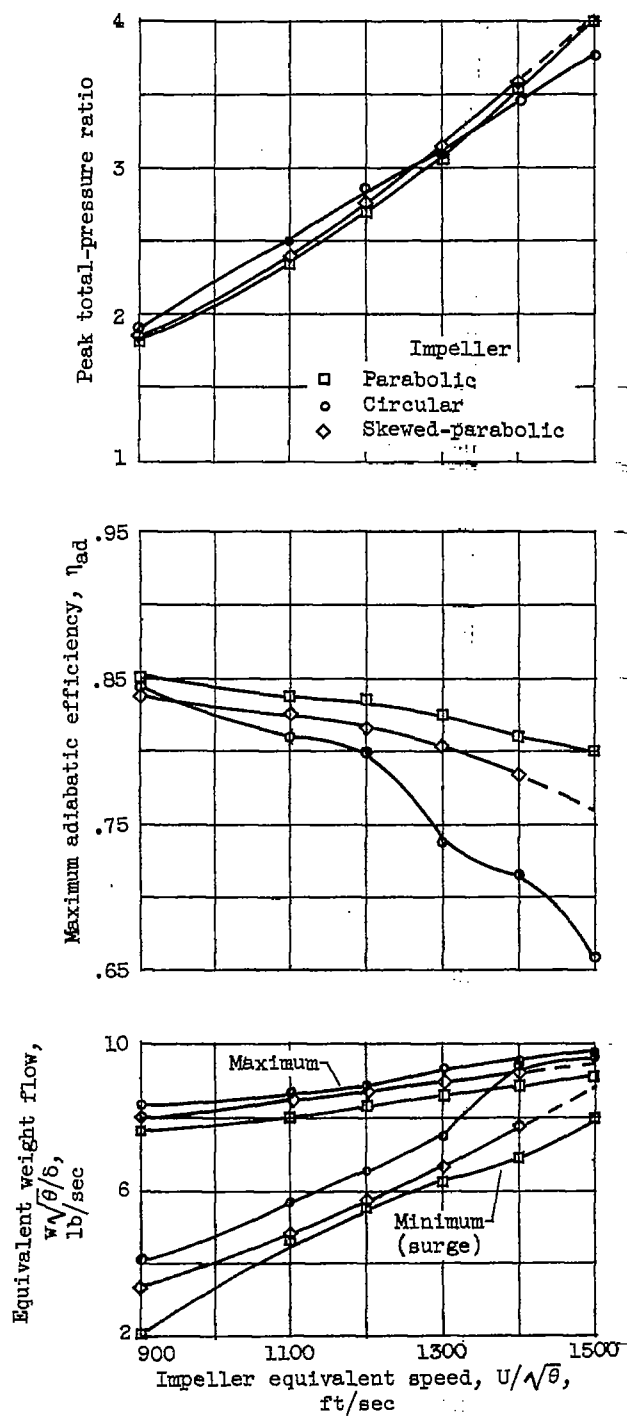


Figure 12. - Comparison of performance of modified parabolic-, circular-, and skewed-parabolic-bladed impellers.